Astron. Astrophys. 239, 356–366 (1990)

ASTRONOMY AND ASTROPHYSICS

Dependence of the properties of solar magnetic flux tubes on filling factor

II. Results of an inversion approach

I. Zayer [1], S.K. Solanki [1,2], J.O. Stenflo [1], and C.U. Keller [1]

[1] Institute of Astronomy, ETH-Zentrum, CH-8092 Zürich, Switzerland
[2] Department of Mathematics, University of St. Andrews, St. Andrews KY16 9SS, Scotland, UK

Received March 19, accepted June 2, 1990

Abstract. The quantitative dependence of magnetic field strength, temperature and turbulent velocity of solar magnetic elements (small flux tubes) on the magnetic filling factor or magnetic flux is studied. The analysed data include Stokes I and V spectra of 23 different regions observed near solar disk centre.

Carefully selected parameters of the Stokes V profiles of three well suited spectral lines are determined and then inverted, using a least squares technique, to derive the temperature, magnetic field strength and turbulent velocity within the flux tubes. The dependence of flux tube temperature and magnetic field strength on the filling factor is firmly established. In general agreement with previous studies flux tubes are found to become cooler and their field strengths, at a given *optical* depth, to become larger as the filling factor increases. The field strength stratification along the *geometrical* height axis, on the other hand, is very similar for all the investigated regions. The flux tubes in all the observed regions are highly evacuated ($0.09 \leqq \beta(z=0) \leqq 0.4$), suggesting that the convective collapse mechanism leading to the formation of intense flux tubes concentrates the field very efficiently.

Some evidence is also found for a slight decrease of the non-stationary velocity amplitude within flux tubes and of the Stokes V amplitude asymmetry with the filling factor. The Stokes V area asymmetry remains unchanged.

Key words: solar magnetic fields – active regions – faculae – flux tubes – Stokes parameters

1. Introduction

Small magnetic elements are thought to account for over 90% of the total magnetic flux outside of sunspots (e.g. Stenflo 1989). Magnetic flux tubes represent the most successful models of these magnetic elements. The two terms are often used interchangeably in the literature and we shall follow this practice. The determination of the internal temperature and magnetic field structure of flux tubes is of primary importance for the empirical study of solar magnetic fields, since most spectral information is intimately connected to these quantities. Also, an empirical knowledge of the flux tube temperature structure is necessary to understand the relative importance of various mechanisms for the energy balance of magnetic elements or of whole active regions (e.g. wave heating, inhibition of convective energy transport, radiative heating and cooling).

Although considerable progress has recently beem made in the empirical determination of the internal atmospheric structure (temperature, magnetic field strength, velocity, etc.) of flux tubes (see e.g. reviews by Stenflo 1989; Solanki 1990), these efforts have been limited to just a few solar regions due to their reliance on a suitably large sample of carefully selected spectral lines, so that they require not only highly resolved Fourier transform spectrometer (FTS) data, but also considerable computational resources. Therefore, comparatively little is known about how the properties of magnetic elements change with the magnetic filling factor, α, which is defined as the fraction of the observed solar surface covered by strong magnetic fields. This aspect must be investigated if we are to understand the flux tube phenomenon properly. For practical reasons this type of investigation is best carried out with a small number of spectral lines.

The dependence of some flux tube properties on α, or more precisely on Stokes V amplitudes, has previously been studied by Stenflo & Harvey (1985), henceforth called Paper I. They found, for example, that the strength of a simple height-independent field changes by a few hundred G as the filling factor changes by approximately a factor of six. They also showed that stationary velocities within magnetic elements are small for all filling factors. Since no proper temperature diagnostic was included in Paper I and only a Milne-Eddington atmospheric model was considered, which is known to be unreliable in reproducing the thermodynamics (Skumanich & Lites 1987), the dependence of flux tube temperature on α was not investigated. This question was, instead, addressed during other investigations by comparing empirical models of flux tubes in a few regions (less than 5) with different filling factors. These investigations suggested that the flux tube temperature does depend on the filling factor (Solanki & Stenflo 1984, 1985; Solanki 1986; Keller et al. 1990), although they also allowed for other interpretations. A dependence of the flux tube temperature on the filling factor is also expected for theoretical reasons (Schüssler 1987; Knölker & Schüssler 1988).

We improve on the analysis of Paper I by using data from a greater number of regions, by employing considerably more

Send offprint requests to: S.K. Solanki (Swiss address)

realistic models coupled to an inversion procedure and by including improved diagnostics of the temperature and of non-stationary velocity amplitudes in our analysis. We apply the inversion technique of Keller et al. (1990) to the Stokes V profiles of 3 spectral lines lying within 4 Å of each other. With its help we put the filling factor dependence of the field strength and of the temperature on a firm observational footing. We also derive the filling factor dependence of the Stokes V asymmetry and of the non-stationary velocity amplitude within solar magnetic elements.

In Sect. 2 we present the data and the reduction procedure. Since a major part of the data was obtained with the Horizontal Arose Telescope (HAT) and these are the first published results from this instrument after its refurbishment into a Stokesmeter, we briefly describe it as well. Section 3 contains a description of the lines selected for analysis, the extracted line parameters and the diagnostics based thereon. This section also includes a description of the used atmospheric models and a brief summary of exploratory calculations aimed at testing the diagnostics. In Sect. 4 we present the results of the data inversions. We briefly describe a preliminary analysis of centre-to-limb data in Sect. 5. Finally, in Sect. 6 we discuss the results and present our conclusions including a comparison with theoretical studies.

2. Observational data and reduction procedure

2.1. Description of the data and the instrumentation

We use data from three different sources in the present work. This offers us the opportunity of comparing the results and examining their consistency. Firstly, we use those spectra obtained with the FTS attached to the McMath telescope of the National Solar Observatory (NSO) at Kitt Peak, which contain the three chosen Fe I lines, λ 5247.1 Å, λ 5250.2 Å, and λ 5250.6 Å. These spectra have been amply described by Stenflo et al. (1984) and Solanki (1987c). Secondly, we reanalyse the data obtained with the vertical grating spectrometer of the McMath telescope which have been described in Paper I and which we call the SH spectra in the following. Finally, we also include data obtained with the Horizontal Telescope of the Arosa Astrophysical Observatory (HAT)[1], the observing station of the Institute of Astronomy of the ETH. The data consist of simultaneous recordings of the Stokes I and V profiles of the selected lines. A total of 23 spectra obtained in regions of varying filling factor at $\mu = \cos\theta \geqq 0.9$, i.e. with the line of sight nearly perpendicular to the solar surface, are analysed in detail. In addition, a few spectra obtained in very quiet regions at disk centre are used to determine instrumental parameters. Finally, we have also analysed 17 spectra obtained at $\mu < 0.9$.

For the present analysis we only use circularly polarized spectra, i.e., Stokes V profiles. They obtain their contribution, at least to first order, from within the flux tubes only. The superiority of this approach over the more conventional use of Stokes I, i.e., unpolarized spectra, has been amply demonstrated in recent years (cf. reviews by Stenflo 1986, 1989; Solanki 1987a, 1990).

The HAT is a refractor with a focal length of 29.44 m (at 4359 Å), with an unfolged light path in a horizontal corridor of the telescope building. A cœlostat mirror system feeds the objective lens of 25.4 cm diameter, which projects the image onto a wall containing the entrance slit of the Littrow spectrometer. The spectrograph itself consists of a 15 cm diameter Littrow collimator/camera lens having a focal length of 12.5 m and a Babcock grating ruled with 600 lines mm^{-1}. The spectrum is scanned by a photomultiplier mounted behind the exit slit. The polarization package is composed of a piezoelastic modular and a linear analyser and is mounted immediately behind the entrance slit of the spectrograph. Circular polarization is converted into intensity modulated light at the modulation frequency $\omega_{\mathrm{mod}} = 50$ kHz. Stokes I is proportional to the DC signal from the photomultiplier, while Stokes V is proportional to the AC signal at ω_{mod} (Stenflo 1984), which is measured with a lock-in amplifier. Two integrators allow the two Stokes parameters to be measured strictly simultaneously, regardless of sequential signal readout. Solar rotation is compensated for, to keep the observed region within the resolution element during an observation which typically lasts 1.8 h. This period is needed to achieve the desired signal-to-noise ratio by repeated wavelength scans (see Sect. 2.2 for the achieved noise levels).

The analysed data have been observed in the 3$^{\mathrm{rd}}$ diffraction order, which, with an entrance aperture (slit) of $14'' \times 0''.42$, translates to a spectral resolution of approximately 23 mÅ at 5250 Å. A realistic estimate of the spatial resolution element is $2\text{–}5'' \times 15\text{–}20''$, depending on the seeing conditions.

We scan two spectral windows, each centered on two of the four lines around 5250 Å, but we leave out the Cr I line at 5247.6 Å from our present analysis. A typical spectrum at $\mu = 1$ (disk centre) can be seen in Fig. 1.

2.2. Data reduction

The FTS and SH data have been reduced during previous investigations, and the procedure is not redescribed here. The reduction of the HAT data to obtain the desired Stokes parameters from the measured signals involves the following main steps:

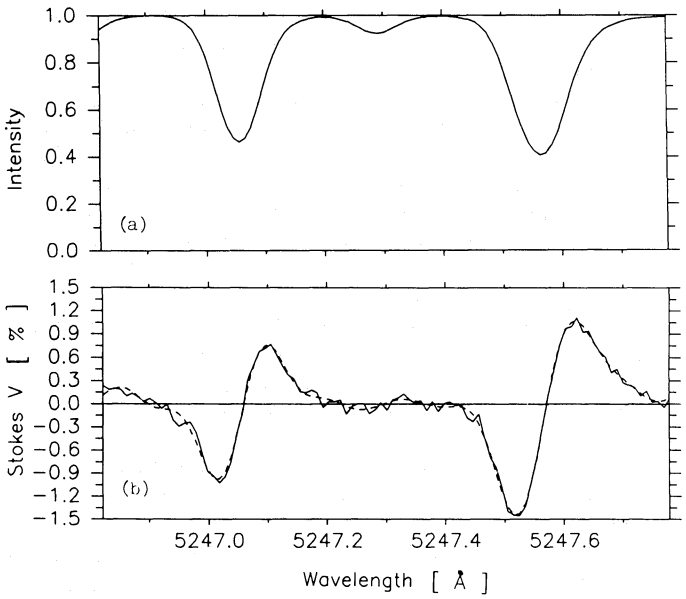

Fig. 1a and b. Typical spectrum of a region at $\mu = 1$ obtained with the HAT. Plotted are the intensity profile, Stokes I (**a**), and the simultaneously recorded circularly polarized Stokes V profile (**b**). The solid curve in **b** represents the originally measured spectrum, the dashed curve is the spectrum after smoothing

[1] The HAT has recently been considerably modernized and upgraded into a Stokesmeter, so that it is now very different from what used to be old HAT.

1. Offsets are first subtracted from the DC and AC signals.

2. To compensate for fluctuations of the atmospheric transmission, the DC signal is divided by a broad-band intensity value recorded simultaneously using a separate photo diode and a third integrator.

3. The brightest (continuum) point of each DC scan is then scaled to unity, resulting in the final normalized Stokes I spectrum of the scan.

4. The degree of polarization (V/I) is obtained from the ratio AC/DC, which is calibrated with the help of a recording made in a non-magnetic region at solar disk centre with a circular polarizer placed in front of the spectrometer slit.

5. Any offset of the polarization zero level caused by instrumental polarization, which is spectrally flat in V/I, is then subtracted. We can safely assume that the true solar polarization in the continuum is smaller than the noise (Kemp 1970; Mürset et al. 1988), and thus determine the offset from the wavelength positions where Stokes $I \geqq 0.98$.

6. Finally, we recover Stokes V through multiplication of the corrected polarization signal by the normalized Stokes I spectrum.

Each repetitive scan of the HAT data can be evaluated individually, or can be added to the others to give the final spectrum with the desired noise level. A slow rotational drift of the grating results in a minute wavelength offset between the individual scans. It is easily compensated for by shifting the scans to make the minimum of a spectral line in a given scan coincide with its minimum in a reference scan. Since we are not interested in the absolute wavelength in the present investigation, this procedure does not affect the results. Since the length of a single scan (approximately 7 min) is incommensurate with the period of the solar global oscillations, adding the scans together should eliminate any profile distortions the oscillations may produce.

We obtain estimates of the instrumental parameters affecting the observed profiles of the HAT and SH data by broadening spectrally resolved, low noise, straylight-free FTS Stokes I spectra until they match the HAT or the SH profiles, respectively. Only data obtained at disk centre in very quiet regions are compared. The effect of the instrumental profile is successfully represented by a convolution with a Gaussian, while the straylight is modelled as a simple additive constant.

For the HAT we find an e-folding width of the Gaussian instrumental profile of $1.3 \pm 0.2\,\mathrm{km\,s^{-1}}$ (the theoretically expected value is $0.95\,\mathrm{km\,s^{-1}}$) and a straylight component of $8.9 \pm 0.8\%$. The corresponding values for the SH data read $1.2 \pm 0.2\,\mathrm{km\,s^{-1}}$ and $11.3 \pm 0.8\%$ which shows that the instrumental parameters of both data sets are comparable and that they can safely be combined in an analysis. We do not deconvolute the observed spectra to account for the effects of instrumental smearing in our model calculations, but rather convolve the calculated synthetic profiles with a Gaussian having the relevant e-folding width. Fortunately, Stokes V is virtually unaffected by straylight in Stokes I. For example, a detailed calculation (Zayer 1989) reveals that the influence of a straylight component of 9% in Stokes I is of the order of 10^{-5} in Stokes V, far below the noise level. Since our analysis only makes use of Stokes V we may neglect the effects of straylight.

We have determined the rms noise level in the observed Stokes V spectra in two different ways: The first method relies on determining the standard deviation (σ) of the continuum points i.e. the points for which $I \geqq 0.98$) from the zero level of Stokes V. Only an upper limit, although a relatively tight one, to the noise level is obtained, since very small real variations in Stokes V due to the haze of very weak lines will be considered part of the noise. The second method is based on Fourier-filtering the high frequency components of the spectrum (e.g. Brault & White 1971) and by comparing the original spectrum with the smoothed one. An idea of the true noise level can be obtained by multiplying the noise level obtained directly from the difference between the two spectra by the fraction $(k_{\max} - 0)/(k_{\max} - k_{\mathrm{cutoff}})$, where $k_{\max}$ ist the maximum wavenumber of the original spectrum (relative to the central fringe) and k_{cutoff} is the wavenumber of the cutoff. Note that this technique can only be applied when the spectrum is considerably oversampled, which is the case for the SH and HAT data. The derived noise levels (absolute rms values) are plotted in Fig. 2. The two techniques give very similar noise levels, with the σ values derived using the second technique actually being somewhat larger. This probably has to do with the cutoff in the high frequency information of the transformed spectrum itself, which causes the V profiles to degrade slightly near their peaks. Therefore, both methods give slightly conservative estimates of the noise. Note that Fig. 2 shows the σ values of all the data points, including those at $\mu < 0.9$.

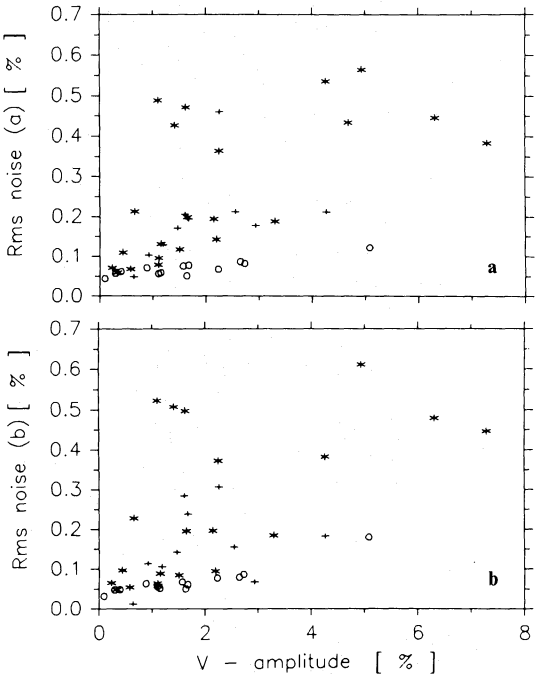

Fig. 2a and b. Rms noise σ of the Stokes V data, determined as described in the text, vs. a_V^{5251}. **a** σ derived using the scatter of the continuum points only. **b** σ derived from the complete spectra using the Fourier smoothing technique. Stars represent HAT data, circles SH observations and crosses the FTS measurements

3. Analysis procedure and model calculations

3.1. *Selected spectral lines and line parameters*

The three lines used for the present investigation consist of the well known Fe I line pair λ 5247.06 Å ($g_{\mathrm{eff}} = 2$, $\chi_e = 0.09$ eV, $\log g^* f = -4.946$, Blackwell et al. 1979) and λ 5250.22 Å ($g = 3$, $\chi_e = 0.12$ eV, $\log g^* f = -4.938$, Blackwell et al. 1979), first introduced for magnetic field strength measurements by Stenflo (1973), and the neighbouring Fe I λ 5250.65 Å line ($g_{\mathrm{eff}} = 1.5$, $\chi_e = 2.2$ eV, $\log g^* f = -2.12$, Thévenin, 1989). Here g is the Landé factor of a Zeeman triplet, g_{eff} the effective Landé factor of an anomalously

split line, χ_e is the excitation potential of the lower level of the transition and g^*f is the statistically weighted oscillator strength. Note the difference of the excitation potentials of λ 5247.1 Å and λ 5250.6 Å. It is responsible for the different temperature sensitivities of the two lines.

We have determined the following parameters from Fourier smoothed V profiles of each line: the amplitudes ($a_{b,r}$), areas ($A_{b,r}$) and full widths at half maxima (FWHM, $\delta\lambda_{b,r}$) of the blue (b) and red (r) wings of the Stokes V profile, respectively. For the further analysis, the averages of the amplitudes, areas and widths of the two V-wings, $a_V=(a_b+a_r)/2$, $A_V=(A_b+A_r)/2$ and $\delta\lambda_V=(\delta\lambda_b+\delta\lambda_r)/2$, are formed and further parameters are calculated from the ones derived above: the relative amplitude and area asymmetries, δa_V and δA_V, defined as $\delta a_V=(a_b-a_r)/(a_b+a_r)$ and $\delta A_V=(A_b-A_r)/(A_b+A_r)$, the magnetic line ratio (MLR), defined as $(2a_V^{5250.2})/(3a_V^{5247})$, and the thermal line ratio (TLR), defined as $(1.5a_V^{5247})/(2a_V^{5250.6})$.

We first test the sensitivities of a selection of the above line parameters to various model parameters. These test calculations are briefly summarized in Sect. 3.4. A final choice of 5 observables, MLR, TLR and $\delta\lambda_V^{1,2,3}$ (the superscripts 1, 2, 3 refer to λ5247.1 Å, λ5250.2 Å and λ 5250.6 Å, respectively) is made as a result of these tests. The chosen line parameters are referred to as observables in the following, and we determine a set of model parameters by an inversion of the observables for each observed region. In addition, we have also analysed the asymmetry of the Stokes V profiles of the three lines $\delta a_V^{1,2,3}$ and $\delta A_V^{1,2,3}$ (superscripts as above).

Of the various filling factor (α) or magnetic flux indicators available, we have chosen one that is relatively little affected by thermal and field strength effects, namely $a_V^{5250.6}$. Note, however, that the relationship between $a_V^{5250.6}$ and α still depends, among other things, on the temperature and the continuum intensity of the flux tubes. If these flux tube parameters themselves depend on α then the relationship between $a_V^{5250.6}$ and α is non-linear. We remove part of this uncertainty by comparing the $a_V^{5250.6}$ of the best fit synthetic profiles to the observed $a_V^{5250.6}$ once the inversion of the data is complete. However, the uncertainty in the continuum intensity within magnetic elements still leaves a residual uncertainty in α (cf. Schüssler & Solanki 1988), as does the possibility of inclined fields (Solanki et al. 1987; Lites & Skumanich 1990) or of a partial cancellation of polarities in the resolution element.

3.2. *Dependence of the extracted observables on Stokes V amplitude*

To obtain a rough idea of the possible dependence of flux tube parameters on α, we have plotted the dependence of the observed line ratios on $a_V^{5250.6}$ in Fig. 3. Figure 3a shows the magnetic line ratio, Fig. 3b the thermal line ratio.

Both line ratios show some dependence on $a_V^{5250.6}$. Also plotted are the best fit straight lines to the data, if the data points are weighted by $1/\sigma$. The lines are described by MLR = $0.763-0.011\cdot a_V^{5250.6}$ and TLR = $0.546-0.020\cdot a_V^{5250.6}$, where $a_V^{5250.6}$ is in % polarization. The scatter of the data points is approximately what is to be expected from the σ values derived in Sect. 2.2, suggesting that for relatively low spatial resolution data, at least, flux tube properties depend mainly on α and not on other parameters in which the present randomly chosen sample may differ (e.g., polarity, age or size of active region, etc.), although other dependences cannot be completely ruled out. Note also that the data from all three instruments, including the FTS, exhibit a consistent behaviour. This contradicts Paper I, where the MLR of the FTS measurements was found to fall distinctly below that of the SH data. This seeming inconsistency between the two investigations may be due to the different methods of noise filtering used. In Paper I a "clean" V profile was produced by scaling the relatively noise-free Stokes V profiles observed in regions with large flux to fit noisy Stokes V profiles and deriving the V amplitudes used to construct the MLR from these scaled profiles. The physically more realistic and less model dependent Fourier filtering method used here is free from the uncertainties and biases of that method.

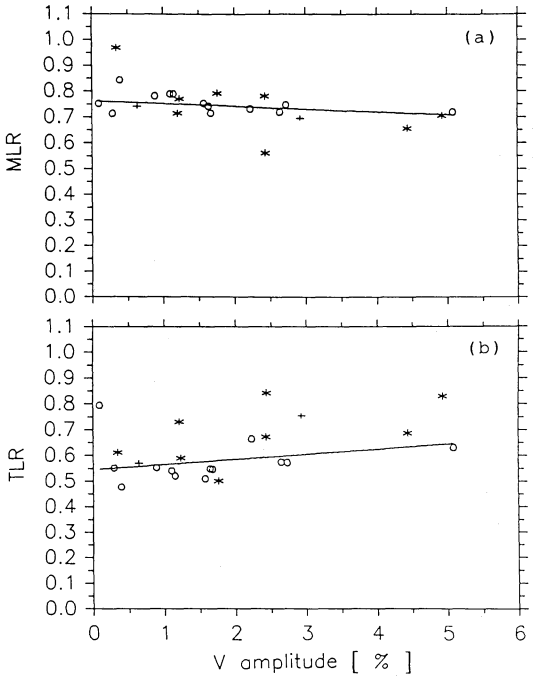

Fig. 3a and b. Dependence of the line rations on $a_V^{5250.6}$ for all the data sets, HAT (stars), SH (circles), and FTS (crosses), is plotted. The individual panels illustrate the magnetic line ratio, MLR (**a**), and the thermal line ration, TLR (**b**). The best linear fits to the data weighted by $1/\sigma$ are also plotted

Recently considerable progress has been made in understanding the origin of the Stokes V asymmetry discovered by Stenflo et al. (1984) and its importance as a diagnostic for, in particular, the temperature and velocity of the surroundings of flux tubes has become clear (Grossmann-Doerth et al. 1988, 1989; Sánchez Almeida et al. 1989; Solanki 1989). However, the dependence of δa and δA on α is still not properly known. We therefore plot δa and δA in Fig. 4, but do not attempt to reproduce them with any model calculations, since this would require dynamic models, which are beyond the scope of the present paper. Fig. 4a shows the Stokes V relative amplitude asymmetry of all three lines for all the solar regions at $\mu\geqq 0.9$ as a function of $a_V^{5250.6}$ (λ 5247.1 Å is represented by stars, λ 5250.2 Å by circles and λ 5250.6 Å by crosses). The solid, dashed and dotted lines represent general trends (smoothed spline interpolarion) for lines λ 5247.1 Å, λ 5250.2 Å, and λ 5250.6 Å, respectively. The data indicate a slight and noisy decrease in the asymmetry with increasing flux. The relative area asymmetry, shown in Fig. 4b, shows no dependence on the filling factor.

3.3. *Models and their parameterization*

Synthetic profiles are calculated with the radiative transfer code described by Solanki (1987c), which is based on an earlier code by

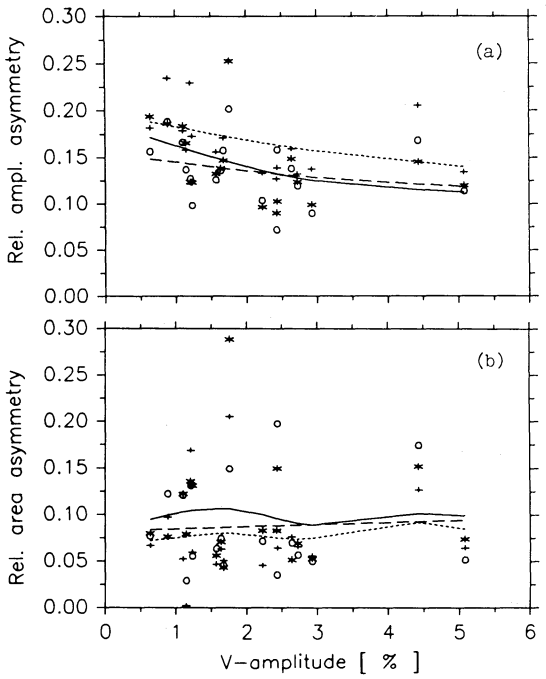

Fig. 4a and b. Relative Stokes V amplitude (**a**) and area (**b**) asymmetries as functions of $a_V^{5250.6}$. Also plotted are spline fits to the data. Stars and the solid line represent λ 5247.1 Å, circles and the dashed line represent λ 5250.2 Å, plusses and the dotted line represent λ 5250.6 Å

Beckers (1969). This is first used to test the dependence of the various observables on model parameters. Then the temperature, magnetic field strength and non-stationary velocity amplitudes are derived for each observed solar region by carrying out a least squares fit of synthetic to observed line parameters (observables). Details of this inversion procedure have been described by Keller et al. (1990).

Since we are restricted to a maximum of five free parameters for the inversion by the chosen number of observables, a stringent parameterization of the physical quantities within the flux tube is needed.

The magnetic field is calculated using the thin tube approximation, which agrees well with observations and with more detailed models (see Zayer et al. 1989; Knölker et al. 1988; Steiner & Pizzo 1989). The field is parameterized in all cases by its value at $\tau = 0.01$. This is the only free parameter needed to describe the magnetic field strength at all heights. Following Solanki (1986), the velocity broadening of the synthetic profiles is modelled using the concept of micro- and macro-turbulence. The microturbulence is kept fixed at $0.6\,\mathrm{km\,s^{-1}}$, while the Gaussian macroturbulence velocity distribution is described by its e-folding width, ξ_{mac}. Since λ 5247.1 Å and λ 5250.2 Å are sufficiently similar to warrant the same macroturbulence broadening (cf. Solanki et al. 1987) only two free parameters are required, $\xi_{\mathrm{mac\,1}}$ for λ 5247.1 Å and λ 5250.2 Å, and $\xi_{\mathrm{mac\,2}}$ for λ 5250.6 Å.

We have attempted to parameterize the temperature in a number of different ways. The most successful of these attempts (as judged from the χ^2 values) has been to assume a geometrical height independent temperature difference, ΔT, with respect to an existing reference model. It is, therefore, the only model whose results we discuss in detail in this paper. It is first used for synthetic profile calculations along a single ray corresponding to the flux tube axis of symmetry (1-D radiative transfer calculations). Later some inversions are also carried out using 1.5-D, i.e. multi-ray, radiative transfer. In this case a series of equidistant, vertical rays are passed through the model flux tube which expands with height to satisfy the conservation of magnetic flux in the presence of a field strength decreasing with height. The line profiles are calculated along each ray, weighted according to the solar surface area it represents, and added together to give a final profile that is compared with the data. The atmosphere surrounding the flux tubes is kept fixed and is given by the modified VAL/SP model described below.

The reference flux tube model used for the major part of our inversion analysis is the plage model of Keller et al. (1990), which is the result of an inversion of 10 Stokes V line profiles (including the three used in the present investigation) observed with an FTS in an active region plage near disk centre. It satisfies hydrostatic equilibrium. It is also quite similar to the plage model of Solanki (1986) derived from the same spectrum using more spectral lines, but a simpler technique. Note that by applying the temperature parameterization described above, with the plage model of Keller et al. (1990) as the reference model, and by choosing an appropriate ΔT we can approximately reproduce the network model of Keller et al. (1990). Therefore the simple temperature parameterization introduced above can be regarded as a rough interpolation between the temperature structures of magnetic elements in regions of quite different filling factors.

To remain consistent with the flux tube model, the quiet photosphere model VAL/SP used by Keller et al. (1990) is also used in the present work. It is based on the empirical model of Vernazza et al. (1976) merged in its deeper layers with the convection zone model of Spruit (1977). The quiet sun model was modified to mimic LTE by Keller et al. (1990), so that the temperature stratification above $\log \tau = -4$ is parallel to that of Holweger & Müller (1974). For some calculations we have also chosen this quiet sun model as the reference model for the inversion.

Note that the use of only one line ratio as a proper temperature diagnostic does not allow reliable information on further temperature parameters (e.g. gradients) to be obtained in a straightforward manner (cf. Grossmann-Doerth et al., in preparation, for more details). However, the other line parameters are not entirely independent of temperature; they are often indirectly affected by it. It may therefore be possible to set some crude constraints on the temperature gradient by including a second temperature parameter ΔT_2. Then ΔT_1 and ΔT_2 are the temperature differences at two distinct heights near the upper and lower boundary of the line forming layers. These two parameters, ΔT_1 and ΔT_2, can be combined to give a measure of an "absolute" temperature offset and of the temperature "gradient" represented by their sum and difference, respectively. The reference model chosen for this parameterization is again the plage model of Keller et al. (1990).

3.4. Exploratory calculations

Extensive exploratory calculations of synthetic line profiles have been performed with both self-consistent and non-self-consistent models. At disk centre the influence of changing $T(\tau)$, $B(\tau)$, or ξ_{mac} on the various line parameters, in particular the TLR and MLR, has been investigated. The results agree with the relevant calculations of Solanki et al. (1987), Steiner & Pizzo (1989), and Keller et al. (1990), although there are differences in detail, due, e.g., to the different models used by the various authors. With one exception we do not go into further details here and refer the interested reader to Zayer (1989).

The dependence of both line ratios on, γ, the angle between the line of sight and the magnetic field vector is established by inclining the magnetic field within an otherwise unchanged 1-D flux tube model having $\Delta T = 200$ K and $B(\tau = 0.01) = 1200$ G. The response of the TLR to γ is very weak. The MLR also shows no significant dependence. A similar investigation was carried out for the MLR by Solanki et al. (1987) with a somewhat different model atmosphere (HSRA with a constant field strength $B = 1000$ G). They found a somewhat larger variation (MLR = 0.7 for $\gamma = 0°$ and MLR = 0.83 for $\gamma = 88°$), but unlike us did not include macro-turbulemce broadening, which is required to reproduce the observed V profiles and which tends to diminish variations in the magnetic line ratio. We conclude that the uncertainty in the γ of the observed regions suggested by the observations of Solanki et al. (1987) and Lites and Skumanich (1989), does not significantly affect the results of our inversion. Therefore we assume that $\gamma = 0°$ for all the inversions of data with $\mu \geqq 0.9$.

4. Results of the analysis at disk centre

Our first attempts to fit the data with the temperature stratification of the VAL/SP model as the underlying reference have consistently failed. Although we have insufficient observables for a stringent determination of the temperature gradient (cf. Sect. 3.3), an imposed temperature stratification which differs too strongly from the true value can nevertheless lead to conflicts with the data, due mainly to the non-linear relation between Stokes V and the atmospheric parameters. We conclude that with the chosen free parameters the VAL/SP quiet sun model is not suitable as a reference model for the inversion of Stokes V data and proceed with the plage model of Keller et al. (1990) as the reference.

The results of the data inversion using the plage model as reference are shown in Fig. 5. The individual panels depict the four free parameters, ΔT, $B(\tau = 1)$ [2], $\xi_{\mathrm{mac}\,1}$ and $\xi_{\mathrm{mac}\,2}$, respectively, vs. $a_V^{5250.6}$. Again, stars represent the HAT data, circles SH spectra and crosses FTS measurements. Only those regions are represented which yield sufficiently small χ^2 values. For the other spectra (generally with high noise levels) we do not consider the derived atmospheric parameters to be reliable.

Note the substantial decrease in temperature and the simultaneous increase in the magnetic field strength with increasing filling factor. Also note that $\Delta T < 100$ K for the FTS plage data, i.e. the data originally used to derive the reference model. Furthermore, the network model of Keller et al. (1990) is hotter by ≈ 400 K at the height of line formation ($\tau \approx 0.01$), which is reflected in our ΔT result of the FTS network data. This suggests that the present inversion procedure gives results consistent with those of the more elaborate one of Keller et al. (1990) and increases our confidence in the simpler version of the inversion used here. The deduced macroturbulences $\xi_{\mathrm{mac}1}$ and $\xi_{\mathrm{mac}2}$ decrease slightly with increasing filling factor, although a constant $\xi_{\mathrm{mac}2}$ cannot be completely ruled out. The instrumental broadening for each instrument has been taken into account in Fig. 5. The difference between $\xi_{\mathrm{mac}1}$ and $\xi_{\mathrm{mac}2}$ is also consistent with the difference expected from the results of Solanki (1986) due to differences in line strength and excitation potential.

[2] $B(\tau = 1)$, and not the actual free parameter $B(\tau = 0.01)$, is plotted to allow a comparison with previous investigations. The field strengths at the two levels are uniquely coupled for a given temperature structure.

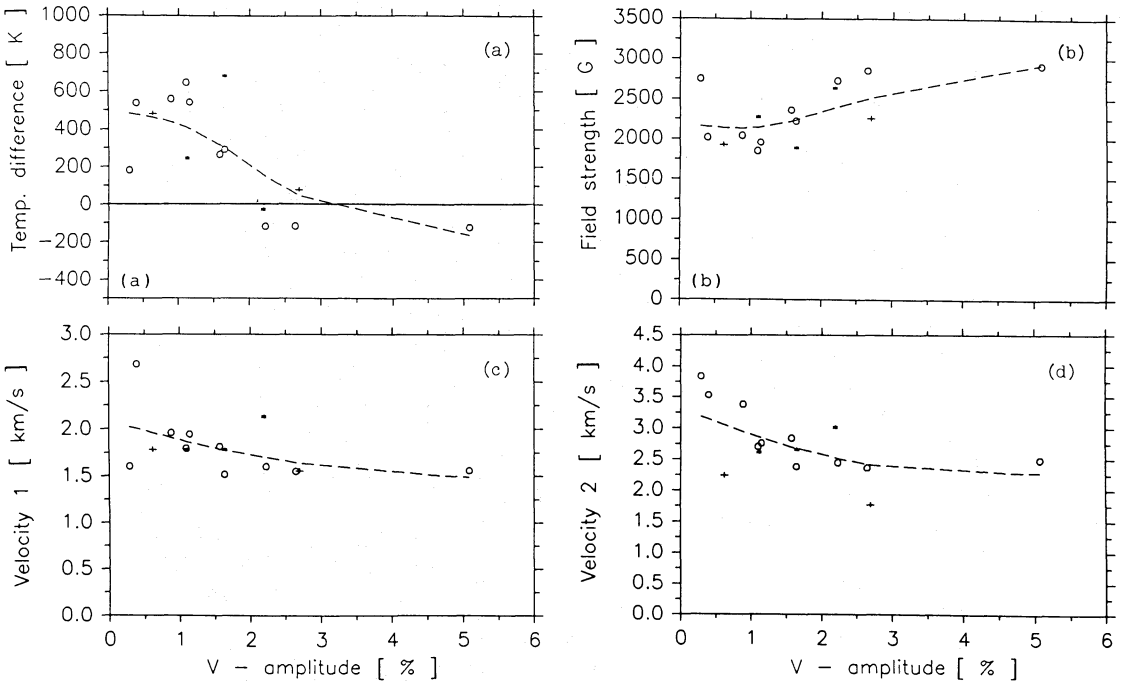

Fig. 5a–d. Results of the Stokes V data inversion. **a** Temperature difference, ΔT, with respect to the reference model (plage model of Keller et al. 1990). **b** Field strength, B, at continuum optical depth $\tau_{5000} = 1$ in the flux tube. **c** Macroturbulence velocity required to broaden λ5247.1 Å and λ5250.2 Å, $\xi_{\mathrm{mac}1}$. **d** Macroturbulence velocity required to broaden λ5250.6 Å, $\xi_{\mathrm{mac}2}$. All quantities are plotted as a function of $a_V^{5250.6}$ (stars: HAT; circles: SH; crosses: FTS). The dashed curves are smoothed spline fits to the data

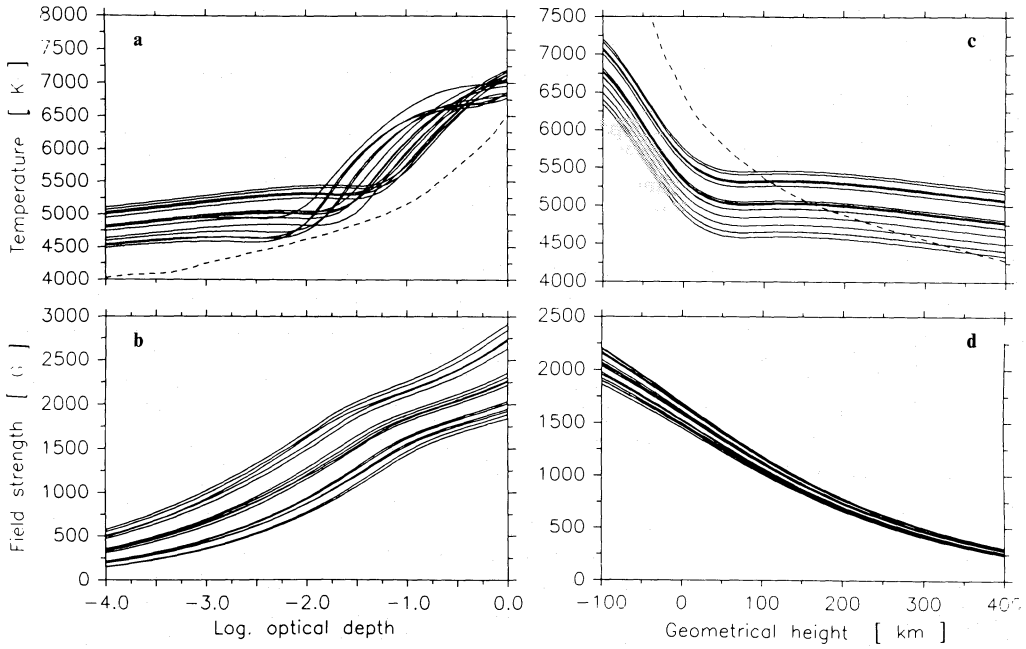

Fig. 6a–d. Temperature (**a**) and field strength (**b**) as functions of $\log(\tau_{5000})$ and temperature (**c**) and field strength (**d**) as functions of geometrical height, z, resulting from the inversion of Stokes V data (solid curves). The dashed curves in **a** and **c** represent the temperature stratification of the quiet sun

It is instructive to consider the behaviour of the temperature and the magnetic field of the best fit models along the continuum optical depth axis, τ_{5000}, and also along the geometrical height axis, z. The temperature $T(\tau)$ and the field strength $B(\tau)$ are plotted in Fig. 6a and b, respectively, while $T(z)$ and $B(z)$ are plotted in Fig. 6c and d, respectively. Each curve in Figs. 6a–d represents the $T(\tau)$, $B(\tau)$, $T(z)$ or $B(z)$ stratification of the best fit model to a particular spectrum.

The $T(z)$ curves simply reflect the temperature parameterization used, i.e. they differ from each other simply by a shift along the T-axis. The difference between the $T(z)$ and the $T(\tau)$ curves is a measure of how strongly the $\tau(z)$ scale (i.e. the continuum opacity) is affected by temperature. Interestingly, *all* the $T(\tau)$ curves remain hotter than the quiet photosphere (dashed curves in Fig. 6a and c) at equal optical depth. The curves of the magnetic field strength $B(z)$ all lie very close together. The relatively small scatter of the $B(z)$ curves derived for the various regions is of the order of magnitude expected from the noise in the data and uncertainties in the inversion procedure (a rough estimate of the uncertainty in $B(z=0)$ due to these two causes is ± 100 G). It therefore appears that magnetic elements have a unique or an almost unique field strength at a given height in the atmosphere. This is due to the strong evacuation of the flux tubes in all the observed regions (see below), so that the derived $B(z)$ curves all resemble the asymptotic case of a completely evacuated flux tube for which $B(z)$ is exclusively determined by the pressure stratification of the external atmosphere. The similarity between the various $B(z)$ curves is in striking contrast to the large variation of $B(\tau)$ in Fig. 6b. The latter is thus clearly induced by changes of the optical depth scale and the heights of formation of the spectral lines due to temperature variations alone. We expect that the clumping of $B(\tau)$ curves into three distinct bands seen in Fig. 6b (and to a certain extent also in Fig. 6d) is caused by insufficient statistics of the observed regions.

Note that the substantial scatter in the $B(\tau)$ curves (Fig. 6b) or in the $B(\tau=1)$ points (Fig. 5b) is much larger than the scatter seen in the field strengths derived using the MLR as the only observable and a height-independent magnetic field model (e.g. using a Milne-Eddington atmosphere, cf. Stenflo 1973; Frazier & Stenflo 1978; and paper I). This apparent discrepancy is resolved if one keeps one major difference in mind. In Fig. 5b B is plotted at the *continuum* optical depth, τ, value unity, while the directly measured quantity is B at optical depth unity in the *spectral line* near the wavelength of the V maximum. If a height-independent B (as in paper I) is assumed then only the latter quantity can be determined. Now, temperature sensitive spectral lines (such as Fe I 5247.1 Å and 5250.2 Å) are formed at different τ values for different temperature stratifications. Since the lines are weakened and therefore formed at a larger τ when the temperature is higher the change in heights of formation effectively compensates the change in the $\tau(z)$ scale, so that the lines are always formed at approximately the same z value and consequently feel approximately the same field strength. The result that $B(z)$ is practically independent of α throughout our extended data set is also consistent with the results of Keller et al. (1990), who found very similar $B(z)$ for both their plage and their network models.

The highest field strengths recorded (approximately 1700 G at $z=0$, i.e. at $\tau_{\rm ext}=1$) correspond to almost the maximum $B(z)$ value possible, suggesting that the flux tubes are highly evacuated. At $z=0$ for the VAL/SP model used here the maximum B is 1789 G, corresponding to a completely evacuated flux tube. To illustrate the evacuation of the flux tubes, we have plotted in Fig. 7 the plasma β, defined as the ratio of gas pressure to magnetic pressure, $\beta = 8\pi P_i/B^2$, where P_i is the gas pressure in the tube. β vs. z is plotted in Fig. 7 for the reference model (dashed line), the network model of Solanki (1986, dotted line) and two extreme best fit models from our 1.5-D inversions (thick solid lines). Also plotted is the theoretically determined critical β for stability to convective collapse (Spruit & Zweibel 1979, thin solid line).

As mentioned in Sect. 3.3 we have also carried out 1.5-D inversions of several selected spectra. No significant differences between the synthetic observables produced by 1-D and 1.5-D models are seen, and the parameters of the best fit models obtained by the two approaches are practically identical. These inversions confirm the validity of 1-D calculations of Stokes profiles in static model flux tubes at disk centre, in good agreement

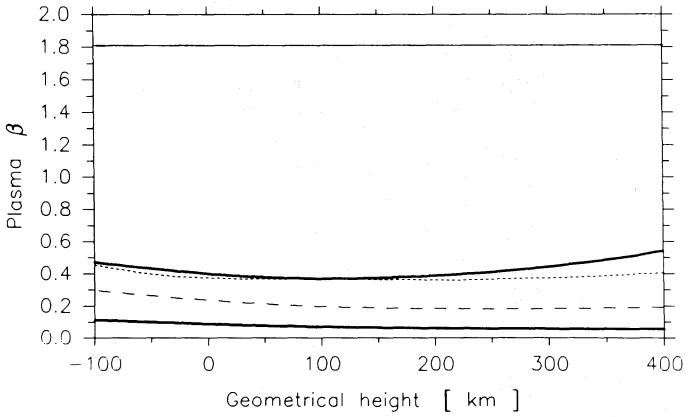

Fig. 7. Plasma β vs. z for the plage model of Keller et al. (1990, dashed curve), the network model of Solanki (1986, dotted curve) and the two best fit models from the 1.5-D inversions with the largest and the smallest $B(z)$ (thick solid curves). Also plotted is the theoretical β limit on convective stability published by Spruit and Zweibel (1979, thin solid curve)

with similar findings by Solanki (1989) and Keller et al. (1990). Note that these conclusions are only valid for solar disk centre.

Once models which can reproduce the observed line profiles have been determined it is possible to obtain a better estimate of the filling factor. In a simple two-component model the filling factor can be determined by comparing the Stokes V amplitudes of the calculated and the observed 5250.6 Å profiles. It is then possible to plot the resulting best fit parameters vs. the estimated filling factor at $\tau = 1$ in the tube directly (Fig. 8, in analogy to Fig. 5). We must, however, add a word of caution to the interpretation of Fig. 8. Since our data do not allow us to obtain any information on the continuum intensity, its variation with filling factor is entirely decided by the simple temperature parameterization of the model. A different behaviour of the continuum intensity within flux tubes with filling factor would distort the filling factor scale in Fig. 8. Note also that due to the expansion of the flux tubes with height, the filling factors at the height of line formation are larger than the α values plotted in Fig. 8.

Finally, let us briefly mention the results of inversions introducing two free temperature parameters. To compensate for the additional free parameters only a single macroturbulence with $\xi_{\mathrm{mac2}} = 1.25\ \xi_{\mathrm{mac1}}$ is used[3]. If we choose the two temperature parameters to be an average temperature enhancement and a difference in temperature gradient at the line forming layers compared to the reference model, then, leaving aside the problems mentioned in Sect. 3.3, we find that the temperature enhancement behaves almost identically to the inversions with only a single temperature parameter ΔT, i.e. it decreases steadily with increasing a_V^{5251}. The temperature gradient, on the other hand, only shows a large scatter and no particular dependence on the filling factor. Interestingly, however, the temperature gradient parameter values tend to be positive, i.e. the temperature gradients of the best fit models tend to be larger than the gradient of the Keller et al. plage model in the line forming layers. The behaviour of the magnetic field and of ξ_{mac} is similar to their behaviour in the case of a single temperature parameter.

[3] As a test we have also inverted the data with a single free thermal parameter, ΔT, and $\xi_{\mathrm{mac2}} = 1.25 \cdot \xi_{\mathrm{mac1}}$. The results are practically identical to the case with two free macroturbulence parameters.

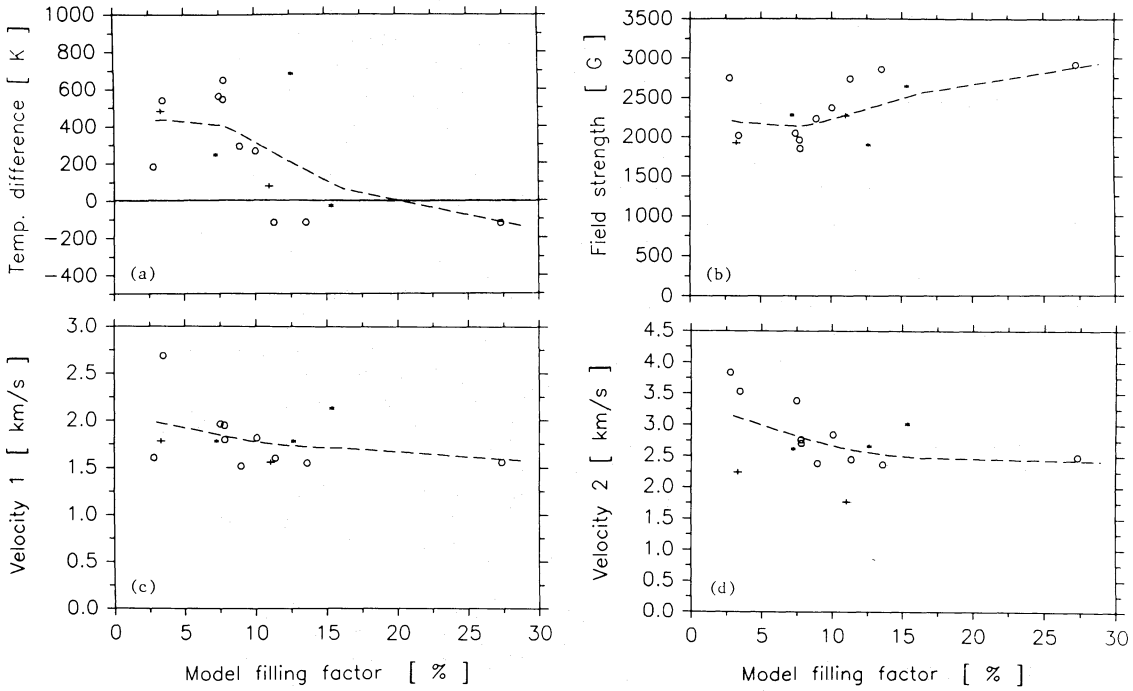

Fig. 8a–d. Results of the data inversion after determination of the model filling factor. **a** Temperature difference, ΔT, with respect to the reference model (plage model of Keller et al. 1990). **b** Field strength $B(\tau_{5000} = 1)$. **c** Macroturbulence velocity required to broaden 5247.1 Å and 5250.2 Å, ξ_{mac1}. **d** Macroturbulence velocity required to broaden 5250.6 Å, ξ_{mac2}. All quantities are plotted as functions of the filling factor derived by comparing the model calculations with the observed profiles (stars: HAT; circles: SH; crosses: FTS). The dashed curves are smoothed spline fits to the data

5. A preliminary centre-to-limb analysis

The HAT was used to obtain a sample of observations covering the (μ, α)-plane to a fair degree. We present here a brief summary of a preliminary analysis of these data. Rather than carrying out an inversion of every single data point, we make use of a regression relation which allows us to reduce the five observables to the case of $\alpha = 0$. The simplest approach consists of assuming a bilinear dependence of the observables on both α and μ. The details of the regression procedure are given by Zayer (1989).

After applying the regression we carry out the inversion for 9 equidistant μ values ranging from 0.2 to 1.0. We employ 2-D models featuring flux conservation in slab geometry. For simplicity and consistency we still call them "flux tubes". Since the flux tube size is no longer arbitrary for $\mu < 1$ we must either use flux tube radii published in the literature (e.g. by Zayer et al. 1989) or derive them again with the reference models used here. We have chosen to redetermine the flux tube width with the technique of Zayer et al. (1989) using the Keller et al. (1990) plage reference model and 1.5-D radiative transfer. We have obtained the following fit parameters for the infrared lines at 15648.5 Å and 15822.8 Å observed at $\mu = 0.61$: $\xi_{\mathrm{mac}} = 3.0\,\mathrm{km\,s^{-1}}$, $B(\tau_{15000} = 1) = 2100\,\mathrm{G}$, and the slab half-width $R_0(\tau_{15000} = 1) = 100\,\mathrm{km}$. The caveats mentioned by Zayer et al. (1989) regarding the value of the flux tube radius determined in this manner are also valid for the present analysis.

The inversion for the 9 μ values is then varried out with $R_0(\tau_{5000} = 1) = 100\,\mathrm{km}$. For $\mu > 0.6$ the results are similar to those expected from the disk centre analysis. However for $\mu < 0.6$ $B(\tau = 1)$ increases considerably with decreasing μ (ΔT remains consistently approximately 200 K). Taken at face value this would suggest that the magnetic field decreases much less rapidly with height than in our reference model, or that it even increases with height which, however, is unphysical. It should also be stated that the fits fail to reproduce the observations for $\mu < 0.4$. There are various possible explanations for these problems:

1. The flux tubes in the observed regions are not vertical, which may have to do with the selection effects mentioned by Stenflo et al. (1987).

2. Near the limb, flux tubes are not observed singly, but rather a single ray may pass though a number of flux tubes. Models composed of arrays of flux tubes will then have to be considered, rather than a single tube as at present (cf. Walton 1987).

3. The average radius of the flux tubes observed in the infrared does not correspond to the average radii in the regions observed in the visible for which the inversions were carried out.

4. The plage model of Keller et al. (1990) is unreliable in the upper photosphere.

At present we cannot reliably distinguish between these possibilities, although some simple preliminary test calculations suggest that points 1 and 2 may hold the key to the resolution of the problems encountered in the centre-to-limb analysis (Zayer 1989).

6. Conclusions

We have studied the dependence of the properties of solar magnetic elements on the magnetic filling factor using Stokes V spectra of 3 lines (Fe I λ 5247.1 Å, λ 5250.2 Å, and λ 5250.6 Å) observed near solar disk centre. We have applied the inversion technique developed by Keller et al. (1990) to these three neighbouring spectral lines and have quantitatively determined the average temperature difference to an existing model atmosphere, the magnetic field strength and the non-stationary velocity in the relevant line forming layers.

We now summarize the main results and list the conclusions drawn from them. Note that the data have been obtained by three different instruments and the reasonable consistency in the behaviour of the extracted observables and the model parameters derived from the three different sources is encouraging.

We provide quantitative evidence for the dependence of the temperature within flux tubes on the amount of magnetic flux. Our results confirm and extend the earlier observational indications of such a dependence which were based on observations of far fewer solar regions and a smaller α range (Solanki & Stenflo 1984, 1985; Solanki 1986; Pantellini et al. 1988; Keller et al. 1990). Theoretical model calculations by Knölker & Schüssler (1988) suggest that there are two possible explanations. Firstly, their models show that flux tubes grow cooler and darker with increasing size. A decrease in temperature with α may, therefore, be due to a greater average size of flux tubes in regions with more magnetic flux. They also argue that flux tubes should be cooler in regions of larger magnetic flux due to the denser packing, even if their size remains unaltered [see Schüssler (1987) and Knölker & Schüssler (1988) for a more detailed discussion of the relevant theoretical ideas]. Unfortunately, the present data cannot easily distinguish between the two proposed mechanisms. We expect that only observations which can determine the the average flux tube size in regions of different flux can resolve this question. For example, very high resolution observations, or a sophisticated CLV analysis of the type carried out by Zayer et al. (1989) may distinguish directly between the two mechanisms. The Zayer et al. (1989) result that all flux tubes have a similar size in a network region observed at $\mu = 1$ supports the second theory, but their technique still needs to be refined considerably and applied to many more regions. The fact that $T(\tau)$ in the flux tubes is always higher than in the quiet sun for all the regions we have analysed (Fig. 6a) also suggests that the flux tubes are rather small even in regions of relatively large filling factor (cf. Knölker & Schüssler 1988).

We reconfirm the presence of kilogauss field strengths within flux tubes. $B(\tau_{5000} = 1)$ varies approximately from 2000 to 3000 G as the Stokes V amplitude of 5250.6 Å increases from 0.1% to 5% (here we do not consider the weak field component detected in infrared spectra by Zayer et al., 1989). However, B at the height of line formation changes considerably less (Paper I) and the field strength as a function of geometrical height, $B(z)$, hardly varies at all with α. Since the temperature stratification changes with the filling factor, the variation of $B(\tau)$ with α is a simple consequence of the α independent $B(z)$ structure and the varying temperature stratification.

Note that $B(\tau)$ and $B(z)$ are model dependent, in the sense that models with other $T(\tau)$ or $T(z)$ *gradients* would lead to changes in the heights of formation of spectral lines which in turn might result in other $B(\tau)$ and $B(z)$ of the best fit models (Grossmann-Doerth et al., in preparation). Consequently, our analysis supports the conclusion of Steiner and Pizzo (1989), that if a model with a *consistently calculated, height dependent* magnetic field strength is used, then diagnostics of both the magnetic field strength and the temperature must be employed concurrently to derive the field strength reliably (compare with Fig. 6b). This is mainly due to the fact that although the MLR (magnetic line ratio) itself is practically temperature independent in the presence of a given height *in*dependent field strength (Solanki et al. 1987), the optical

depths of formation of the two lines (5247.1 Å and 5250.2 Å) depend strongly on the temperature structure (Grossmann-Doerth et al., in preparation). Since the magnetic field strength varies with height, the MLR will also change with changing temperature (cf. Steiner & Pizzo 1989).

Leaving such uncertainties aside for the moment (the similarity to the result of Keller et al. 1990, suggests that they are not too significant, anyway), the $B(z)$ observations do provide a new, tighter, observational constraint on any theoretical models predicting field strengths of magnetic elements. The main constraint is that the flux tubes are strongly evacuated (Fig. 7), suggesting that the mechanism responsible for the concentration of the field, namely convective collapse, is highly efficient. Various convective collapse calculations have been published (e.g. Parker 1978; Webb & Roberts 1978; Spruit & Zweibel 1979; Spruit 1979; Venkatakrishnan 1983; Hasan 1984, 1985, 1990; see also the reviews by Solanki 1987b; Schüssler 1990; Thomas 1990). Linear stability analysis (Webb & Roberts 1978; Spruit & Zweibel 1979) allows a lower limit of approximately 1200–1300 G at $z=0$, corresponding to $\beta=1.8$, to be set on the field strength of stable tubes. Calculations of the non-linear development of the collapsed state give field strengths comparable to the observations, but allow a much too large range of stable field strengths to exist $1280\,\mathrm{G} \simeq B(z=0) \lesssim 1650\,\mathrm{G}$ (Spruit 1979). According to these calculations a smaller range of field strengths at $z=0$ can be produced if the initial (pre-collapse) field strength also lies in a very narrow range. However, all these calculations make an invalid assumption, namely that β is heigth independent which implies that the temperature inside the tube is exactly equal to the outside temperature at equal geometrical height, a condition our results show to be manifestly not fulfilled. Unfortunately even the most detailed convective collapse calculations (non-linear, with vertical radiative transfer in the Eddington approximation, Hasan 1990) give a time-averaged field strength of approximately 1300 G at $z=0$ instead of 1600 G, i.e. the calculated convective collapse is not sufficiently efficient in concentrating the field. Evidently the models must be refined further. See also the review by Schüssler (1990) for a critical appraisal of current convective collapse calculations from a physical point of view.

We confirm that 1-D radiative transfer is an accurate approximation for line formation in flux tubes at $\mu=1$, as long as we only consider static models and are not interested in the asymmetry of Stokes V (Solanki 1989) and as long as the calculated lines are not fully Zeeman split (Zayer et al. 1989).

The amplitude of the non-stationary velocity, ξ_{mac}, within magnetic elements is found to decrease somewhat with increasing filling factor. There are two possible explanations for this: 1. The flux tubes in regions with larger α expand faster with height, so that the velocity amplitude of disturbances excited in the convection zone within the tube cannot grow so fast with height (energy conservation). This would reduce the velocity amplitude at the level of line formation for a given wave energy flux produced in the convection zone. 2. Disturbances are not excited as strongly within tubes in regions of large magnetic flux. The first explanation can be ruled out, since it is the hotter tubes which fan out faster with height (cf. e.g. Steiner & Pizzo 1989; Solanki & Steiner 1990), so that if this were the main effect, we would observe an increase in velocity amplitude with filling factor. Therefore, the excitation mechanism of disturbances must be reduced in regions with larger α. One of the main proposed mechanisms for longitudinal wave generation is the compression of flux tubes by neighbouring granules (e.g. Musielak et al. 1989). Observations from Spacelab II do indeed suggest that both the steady and the fluctuating components of the horizontal velocity of granules in active regions are supressed and the granule lifetimes extended (Title et al. 1989), so that the efficiency of this mechanism is expected to be reduced as α increases.

The area asymmetry of Stokes V remains unaffected by the filling factor. This agrees with the calculations of the Stokes V asymmetry by Solanki (1989) using 2-D flux tube models. However, the observations indicate a slight decrease of the Stokes V amplitude asymmetry, δa with increasing filling factor. The decrease is well correlated to the behaviour of ξ_{mac}. A correlation between δa and ξ_{mac} is expected if δa is partly due to non-stationary velocities within the flux tubes, as suggested by Solanki (1989). The validity of this mechanism is therefore reinforced by the present analysis.

Acknowledgements. We are deeply indepted to H.P. Povel for the implementation and a major part of the design of the hardware and software for the telescope controller and the polarimeter. F. Aebersold carried out the mechanical refurbishment of the HAT with great skill and precision. F. Reufer helped with the software development for the HAT controller. M. Schüssler critically read and commented on the manuscript. Their contributions are gratefully acknowledged. The work of I.Z. and C.K. was supported by grants No. 2.666-0.85, 2.417-0.87, and 2000-5.229 from the Swiss National Science Foundation.

References

Beckers, J.M., 1969, Solar Phys. 9, 372
Blackwell, D.E., Ibbetson, P.A., Petford, A.D., Shallis, M.J., 1979, MNRAS 186, 633
Brault, J.W., White, O.R., 1971, A&A 13, 169
Frazier, E.N., Stenflo, J.O., 1978, A&A 70, 789
Grossmann-Doerth, U., Schüssler, M., Solanki, S.K., 1988, A&A 206, L37
Grossmann-Doerth, U., Schüssler, M., Solanki, S.K., 1989, A&A 221, 338
Hasan, S.S., 1984, ApJ 285, 851
Hasan, S.S., 1985, A&A 143, 39
Hasan, S.S., 1990, in Proc. Chapman Conference on Magnetic Flux Ropes, eds. C.T. Russell, E.R. Priest, L.C. Lee, Geophysical Monograph 58, American Geophysical Union, Washington, p. 157
Holweger, H., Müller, E.A., 1974, Solar Phys. 39, 19
Keller, C.U., Solanki, S.K., Steiner, O., Stenflo, J.O., 1990, A&A 233, 583
Kemp, J.C.: 1970, ApJ 162, 169
Knölker, M., Schüssler, M., 1988, A&A 202, 275
Knölker, M., Schüssler, M., Weisshaar, E., 1988, A&A 194, 257
Lites, B.W., Skumanich, A., 1990, ApJ 348, 747
Mürset, U., Solanki, S.K., Stenflo, J.O., 1988, A&A 204, 279
Musielak, Z.E., Rosner, R., Ulmschneider, P., 1989, ApJ 337, 470
Pantellini, F.G.E., Solanki, S.K., Stenflo, J.O., 1988, A&A 189, 263
Parker, E.N., 1978, ApJ 221, 368
Sánchez Almeida, J., Collados, M., Del Toro Iniesta, J.C., 1989, A&A 222, 311
Schüssler, M., 1987, in The Role of Fine-Scale Magnetic Fields on the Structure of the Solar Atmosphere, eds. E.-H. Schröter, M. Vázquez, A.A., Wyller, Cambridge University Press, Cambridge, p. 223

Schüssler, M., 1990, in Solar Photosphere: Structure, Convection, Magnetic Fields, ed. J.O. Stenflo, IAU Symp. 138, 161
Schüssler, M., Solanki, S.K., 1988, A & A 192, 338
Skumanich, A., Lites, B.W., 1987, ApJ 322, 473
Solanki, S.K., 1986, A & A 168, 311
Solanki, S.K., 1987a, in The Role of Fine-Scale Magnetic Fields on the Structure of the Solar Atmosphere, eds. E.-H. Schröter, M. Vázquez, A.A. Wyller, Cambridge University Press, Cambridge, p. 67
Solanki, S.K., 1987b, in Proc. Tenth European Regional Astronomy Meeting of the IAU, Vol. 1, The Sun, eds. L. Hejna, M. Sobotka, Publ. Astron. Inst. Czechoslovak Acad. Sci., p. 95
Solanki, S.K., 1987c, Ph.D. Thesis, No. 8309, ETH, Zürich
Solanki, S.K., 1989, A & A 224, 225
Solanki, S.K., 1990, in Solar Photosphere: Structure, Convection, Magnetic Fields, ed. J.O. Stenflo, IAU Symp. 138, 103
Solanki, S.K., Keller, C., Stenflo, J.O., 1987, A & A 188, 183
Solanki, S.K., Steiner, O., 1990, A & A 234, 519
Solanki, S.K., Stenflo, J.O., 1984, A & A 140, 185
Solanki, S.K., Stenflo, J.O., 1985, 148, 123
Spruit, H.C., 1977, Ph.D. Thesis, Univ. Utrecht
Spruit, H.C., 1979, Solar Phys. 61, 363
Spruit, H.C., Zweibel, E.G.,1979, Solar Phys. 62, 15
Steiner, O., Pizzo, V.J., 1989, A & A 211, 447
Stenflo, J.O., 1973, Solar Phys. 32, 41
Stenflo, J.O., 1984, Appl. Optics 23, 1267
Stenflo, J.O., 1986, in Small Scale Magnetic Flux Concentrations in the Solar Photosphere, eds. W. Deinzer, M. Knölker, H.H. Voigt, Vandenhoek & Ruprecht, Göttingen, p. 59
Stenflo, J.O., 1989, A & AR 1, 3
Stenflo, J.O., Harvey, J.W., 1985, Solar Phys. 95, 99 (Paper I)
Stenflo, J.O., Harvey, J.W., Brault, J.W., Solanki, S.K., 1984, A & A 131, 333
Stenflo, J.O., Solanki, S.K., Harvey, J.W., 1987, A & A 173, 167
Thévenin, F., 1989, A & AS 77, 137
Thomas, J.H., 1990, in Proc. Chapman Conference on Magnetic Flux Ropes, eds. D.T. Russell, E.R. Priest, L.C. Lee, Geophysical Monograph 58, American Geophysical Union, Wahington, p. 133
Title, A.M., Tarbell, T.D., Topka, K.P., Fergusen, S.H., Shine, R.A., and the SOUP Team, 1989, ApJ 336, 475
Venkatakrishnan, P., 1983, JA & A 4, 135
Vernazza, J.E., Avrett, E.H., Loeser, R., 1976, ApJS 30, 1
Walton, S.R., 1987, ApJ 312, 909
Webb, A.R., Roberts, B., 1978, Solar Phys. 59, 249
Zayer, I., 1989, Ph.D. Thesis, No. 8995, ETH, Zürich
Zayer, I., Solanki, S.K., Stenflo, J.O., 1988, A & A 211, 463